PLOS ONE

RESEARCH ARTICLE

The brain anatomy of attention-deficit/hyperactivity disorder in young adults – a magnetic resonance imaging study

Jean-G. Gehricke[1,2]*, Frithjof Kruggel[3], Tanyaporn Thampipop[1,2], Sharina Dyan Alejo[1,2], Erik Tatos[1,2], James Fallon[4], L. Tugan Muftuler[5]

1 Department of Pediatrics, University of California, Irvine, Irvine, California, United States of America, **2** The Center for Autism & Neurodevelopmental Disorders, Santa Ana, California, United States of America, **3** Department of Biomedical Engineering, University of California, Irvine, Irvine, California, United States of America, **4** Department of Anatomy & Neurobiology, University of California, Irvine, Irvine, California, United States of America, **5** Department of Neurosurgery, Medical College of Wisconsin, Milwaukee, Wisconsin, United States of America

* jgehrick@uci.edu

Citation: Gehricke J-G, Kruggel F, Thampipop T, Alejo SD, Tatos E, Fallon J, et al. (2017) The brain anatomy of attention-deficit/hyperactivity disorder in young adults – a magnetic resonance imaging study. PLoS ONE 12(4): e0175433. https://doi.org/10.1371/journal.pone.0175433

Editor: Linda Chao, University of California, San Francisco, UNITED STATES

Received: October 26, 2016

Accepted: March 24, 2017

Published: April 13, 2017

Data Availability Statement: All relevant data are within the paper and its Supporting Information files.

Funding: This investigation was supported by grant K01 DA25131 to Jean-G. Gehricke from the National Institute on Drug Abuse of the National Institutes of Health. In addition, the project was supported by the National Center for Research Resources and the National Center for Advancing Translational Sciences, National Institutes of Health, through grants RR00827 and UL1

Abstract

Background

This is one of the first studies to examine the structural brain anatomy and connectivity associated with an ADHD diagnosis and child as well as adult ADHD symptoms in young adults. It was hypothesized that an adult ADHD diagnosis and in particular childhood symptoms, are associated with widespread changes in the brain macro- and microstructure, which can be used to develop a morphometric biomarker for ADHD.

Methods

Voxel-wise linear regression models were used to examine structural and diffusion-weighted MRI data in 72 participants (31 young adults with ADHD and 41 controls without ADHD) in relation to diagnosis and the number of self-reported child and adult symptoms.

Results

Findings revealed significant associations between ADHD diagnosis and widespread changes to the maturation of white matter fiber bundles and gray matter density in the brain, such as structural shape changes (incomplete maturation) of the middle and superior temporal gyrus, and fronto-basal portions of both frontal lobes. ADHD symptoms in childhood showed the strongest association with brain macro- and microstructural abnormalities. At the brain circuitry level, the superior longitudinal fasciculus (SLF) and cortico-limbic areas are dysfunctional in individuals with ADHD. The morphometric findings predicted an ADHD diagnosis correctly up to 83% of all cases.

Conclusion

An adult ADHD diagnosis and in particular childhood symptoms are associated with widespread micro- and macrostructural changes. The SLF and cortico-limbic findings suggest

TR000153, respectively, and the generous financial support of The Center for Autism & Neurodevelopmental Disorders.

Competing interests: The authors have declared that no competing interests exist.

complex audio-visual, motivational, and emotional dysfunctions associated with ADHD in young adults. The sensitivity of the morphometric findings in predicting an ADHD diagnosis was sufficient, which indicates that MRI-based assessments are a promising strategy for the development of a biomarker.

Introduction

Attention-Deficit/Hyperactivity Disorder (ADHD) is characterized by inattention, hyperactivity, and impulsivity. It is one of the most frequently diagnosed neurodevelopmental disorders with a prevalence rate of approximately 5% in children and 2.5% in adults [1]. Estimates suggest that 65% of children with ADHD continue to have problems in adulthood [2]. While ADHD is well-characterized at the behavioral level in children, little is known about the association between brain structure and ADHD diagnosis as well as symptoms across the lifespan.

The most frequently used approaches to measure brain structures are based on Magnetic Resonance Imaging (MRI). T1-weighted anatomical imaging is used to assess the brain macrostructure, such as the volume and structure of white matter (i.e., a high proportion of myelinated axons) and grey matter (i.e., a high proportion of neuronal cell bodies), while diffusion-tensor imaging (DTI) is a more recent approach to specifically assess the brain microstructure. DTI provides information about the mobility of water molecules in white matter via the scalar parameters: fractional anisotropy (FA)–directionality of water diffusion perpendicular to white matter fibers [3]; radial diffusivity (RD)–diffusion rate perpendicular to white matter tracts; axial diffusivity (AD)–diffusion rate parallel to axons; and mean diffusivity (MD), reflecting overall water mobility [4, 5]. Decreases in FA can be associated with increases in MD, which suggests increased extracellular space or decreased axonal density [4]. Alternatively, decreased FA may result from increased RD, indicating decreased myelination [4, 6].

A number of studies documented the macro- and microstructural pathophysiology associated with an ADHD diagnosis. Initial brain macrostructural studies revealed that children and adolescents with ADHD show smaller brain volumes in all regions [7]. However, subsequent meta-analyses [8–11] mainly report differences in basal ganglia together with changes in total brain [8] or gray matter volume [11]. Intriguingly, most volume differences appear to normalize with transition to adulthood [12].

Besides these macrostructural indicators, it was suggested that ADHD primarily involves the fronto-striatal [13] as well as fronto-parietal networks [14]. More specifically, dysregulated functional communications in these networks are assumed to cause the behavioral dysfunction associated with ADHD [15]. A meta-analysis corroborated this notion by revealing that children with ADHD show compromised white matter (WM) integrity in the inferior and superior longitudinal fasciculus, anterior corona radiate, cortico-spinal tract, cingulum, corpus callosum, and the internal capsule and cerebellum [16]. Such compromised WM integrity may contribute to the dysfunctional communication in frontal-striatal and parietal networks. In addition, it was suggested that the pathophysiology of ADHD includes a dysregulated modulation of cortical plasticity during brain development, resulting in an abnormal cortico-cortical connectivity that may persist into adulthood [17]. Some studies support that ADHD is associated with lifelong abnormal connectivity by showing that adults with ADHD have reduced connectivity in the orbito-medial prefrontal cortex, right anterior cingulate, right anterior corona radiata and the superior as well as inferior longitudinal fasciculus among other regions [18–21], and increased MD in the orbito-medial prefrontal cortex, right anterior cingulate, and left fronto-occipital fasciculus [19, 22]. These areas are central for connecting the

prefrontal cortex to the basal ganglia, consisting of caudate and putamen [23], which are smaller in children but not in adults with ADHD [7, 10].

It was suggested that changes in the striatum and its connections are associated with hyperactivity-impulsive symptoms in children with ADHD [16]. However, the size of basal ganglia regions may initially correlate with hyperactive-impulsive symptoms, which decline over time and may disappear during adulthood [24]. This notion was corroborated by showing that the lack of differences in the striatal volumes in adults with ADHD may be caused by reductions in hyperactive-impulsive symptoms in adulthood [25].

In children and adolescents, severity of ADHD symptoms was linked to decreased frontal and temporal grey matter, caudate and cerebellar volumes, [7] and decreased FA [15, 21, 26]. These findings suggest that the prefrontal cortex and its connections may be associated with ADHD symptoms such as distractibility, forgetfulness, impulsivity, poor planning and hyperactivity in both children and adults with ADHD [27]. In children and adolescents with ADHD, inattention was linked to reduced brain connectivity not only in the frontal but also in the anterior cingulate, temporal, and parietal regions [28]. However, the extent of dysfunctional connectivity has yet to be determined in young adults with ADHD. Thus far, the literature suggests that a diagnosis of ADHD as well as ADHD symptoms may be associated with widespread changes in the brain macro- and microstructure. In addition, as many adults with ADHD show symptom improvements [29], the correlations between childhood symptoms and brain macro- and microstructure may weaken in adulthood due to brain maturation or improved coping skills. However, there are no studies that directly examine brain anatomical correlates of ADHD diagnosis as well as child and adult ADHD symptoms in young adults with ADHD.

The purpose of the study was to close this gap in knowledge by analyzing structural and diffusion-weighted MRI data in relation to ADHD diagnosis and the number of self-reported childhood and adult symptoms in young adults. The aim of the study was threefold: 1. to examine macro- and microstructural correlates of an ADHD diagnosis in young adults with ADHD, 2. to study associations between brain structure and child as well as adult symptoms of ADHD, and 3. to assess if the morphometric correlates of ADHD can be used as a potential biomarker to predict an ADHD diagnosis. Based on previous research showing widespread changes in the brain macro- and microstructure, it was hypothesized that an adult ADHD diagnosis is associated with frontal, basal ganglia, anterior cingulate, temporal, and parietal regions in young adults with ADHD. In addition, it was hypothesized that correlations between brain structure and ADHD symptoms in childhood are more widespread and prominent (i.e., number, size, and z-scores of significant brain regions) than ADHD symptoms in adulthood. Moreover, the morphometric findings may predict the ADHD diagnosis in more than 80% of cases, which would demonstrate that morphometric data have the potential to be used as a biomarker for the diagnosis of ADHD.

Methods

Participants

Seventy-two participants participated in the study of which 31 met the diagnostic criteria for ADHD according to DSM-IV [30], and 41 controls without an ADHD disorder (see Table 1). Similar to previous studies [31–34], each participant was assessed according to DSM-IV-TR criteria [30] with the Structured Clinical Interview for DSM-IV (SCID), [35] and the QUEST method [36]. Severity of ADHD symptoms was evaluated using the Assessment of Hyperactivity and Attention (AHA), which is a quantitative measure of ADHD symptomatology [37]. The AHA [37], an 18-item questionnaire, is based on DSM-IV criteria and was used to

Table 1. Participant Sample Characteristics.

Characteristics	ADHD (N = 32)	Control (N = 40)
Ages, Years (M ± SD)	25.31 ± 5.44	23.93 ± 3.60
Male/Female (N)	26/6	33/7
Of European Decent (%)	68.75	62.50
Education, years (M ± SD)	13.28 ± 2.70	15.20 ± 2.36
Employed (%)	56.30	80.00*
ADHD Subtype		
Predominantly Inattentive Subtype (%)	37.50	0.00***
Predominantly Hyperactive/Impulsive Subtype (%)	6.25	0.00
Predominantly Combined Subtype (%)	56.30	0.00***
Number of Childhood ADHD Symptoms (M ± SD)	14.13 ± 3.6	5.83 ± 5.81***
Number of Inattentive Symptoms (M ± SD)	7.56 ± 1.88	3.45 ± 3.20***
Number of Hyperactive/Impulsivity Symptoms (M ± SD)	6.56 ± 2.49	2.38 ± 3.04***
Number of Adult ADHD Symptoms (M ± SD)	9.56 ± 3.885	3.30 ± 3.88***
Number of Inattentive Symptoms (M ± SD)	5.13 ± 2.50	1.98 ± 2.43***
Number of Hyperactive/Impulsivity Symptoms (M ± SD)	4.44 ± 2.26	1.33 ± 1.70***
Number of Participants with Comorbidities (%)	31.25	25.00
Anxiety Disorder (%)	21.90	10.00
Eating Disorder (%)	3.13	2.50
Learning Disorder (%)	0.00	2.50
Mood Disorder (%)	9.38	5.00
Other Substance Use Dependence (%)	9.38	7.50
Current use of Stimulant Medication (%)	25.00	0.00**
Adderall (%)	15.63	0.00**
Ritalin (%)	9.38	0.00*

*$p \leq 0.05$
**$p \leq 0.01$
***$p \leq .001$

https://doi.org/10.1371/journal.pone.0175433.t001

measure severity of both childhood and adult symptoms of ADHD. Although the number of controls who met DSM-VI criteria for ADHD was zero, 21 control participants had at least one ADHD symptom. However, these ADHD symptoms were to low in frequency and did not cause sufficient clinical impairment to warrant a clinical diagnosis of ADHD. Compared to controls, participants with ADHD had lower levels of employment ($\chi^2 = 4.73$, $p = 0.03$), more ADHD symptoms ($t \geq 5.39$, $p \leq 0.0001$) as well as subtype diagnoses ($\chi^2 \geq 18.00$, $p \leq 0.001$), and currently used more stimulant medications ($\chi^2 \geq 3.91$, $p \leq 0.05$).

All participants were physically healthy and had no chronic illness such as heart disease, irregular heartbeat, hypertension, diabetes, skin allergies, or skin diseases. The study was approved by the Institutional Review Board of the University of California, Irvine and written consent was obtained from each participant between July 2009 and April 2014.

Procedure

Participants were asked to close their eyes and relax while in the MRI scanner. The duration of the scan was 20 minutes (i.e., 10 minutes to obtain T1 weighted images and another 10 minutes to obtain diffusion weighted image set).

Imaging protocol

MRI data were acquired on a Philips Achieva 3T scanner, equipped with an 8-channel phased array coil. T1-weighted images were acquired using a Turbo Field-Echo (TFE) sequence with TR 11 ms, TE 3.7 ms, flip angle 18 degrees, 150 sagittal slices with a matrix of 240 x 240 voxels, corresponding to an isotropic resolution of 1.0 mm. Diffusion-weighted images were acquired using a diffusion-weighted spin-echo EPI sequence with TR 7.0 s, TE 80.0 ms, flip angle 90 degrees, 60 axial slices with a matrix of 116 x 112 voxels, corresponding to a resolution of 1.8 mm x 1.8 mm (in plane), 2 mm slice thickness. Thirty-two image volumes were acquired using different diffusion weighting gradient directions at b = 1000 s/mm^2, one volume with isotropic gradients at b = 1000 s/mm^2, and a reference volume without diffusion-weighting (b = 0 s/mm^2).

Processing of T1-weighted images

Data analysis followed the general outline of voxel-based morphometry (VBM). The BRIAN software package was used to analyze the imaging data (http://sip.eng.uci.edu). All T1-weighted MR images were inspected for acquisition-related artifacts and signs of neurological diseases. Heads were aligned with the stereotaxic coordinate system [38] and registered with the ICBM 2009c template [39], using a recent approach for nonlinear registration [40]. All registered head images were scaled for a mean intensity of 100 and averaged. The brain was extracted from the averaged head image to yield the brain template 1. Subsequently, a mask of the intracranial volume was generated from each head dataset and used to extract the intracranial space [41]. Data were corrected for intensity inhomogeneities using a newly developed technique that estimates the gain field by comparing the global and regional intensity distribution. Next, the intensity-corrected image was segmented into three probabilistic maps (roughly corresponding to: cerebrospinal fluid (CSF) grey and white matter). The volume integral of these compartments was used as an estimate of the intracranial volume (ICV). All intensity-corrected brain images were registered with template 1, and averaged to yield the brain template 2. This procedure is considered standard for generating a study-specific template (S1 Template) [42]. The first template depends on properties of the initial atlas, while the second template was generated using information from this study alone. All brain data sets were registered with template 2, and the resulting deformation field applied to the GM (WM) probabilistic map, now interpreted as GM (WM) concentration (GMC, WMC). Finally, these maps were smoothed using a Gaussian filter (σ = 2, FWHM of 4.7 mm) and logit-transformed. From the deformation field obtained above, the determinant of the first partial derivative (the Jacobian) was computed. This value can be used to detect local shape changes (greater than 1 for locally expanding areas, less than one for locally contracting areas, and 1 for no change, translations and rotations). Data were smoothed using a Gaussian filter (FWHM of 4.7 mm), and log-transformed. Thus, maps were obtained for the GM (WM) concentration and Jacobian (JAC) for each subject in normalized space.

Processing of diffusion-weighted images

The BRIAN software package was used to analyze the imaging data (http://sip.eng.uci.edu). To correct for subject motion, image volumes corresponding to all gradient directions were registered with the non-diffusion weighted reference image volume using affine registration and mutual information as an image similarity metric. Then, diffusion tensors were computed from the registered diffusion-weighted images using a nonlinear procedure including anisotropic noise filtering [43]. Tensors were converted into scalar measures fractional anisotropy (FA), radial, mean and axial diffusivity (RD, MD, AD) values. The reference volume of the DTI data set was linearly registered with the T1-weighted brain image obtained above, and the resulting transformation was used to map each measure into stereotaxic space. Next, the

deformation field obtained above was used to warp measures into normalized space. Finally, these maps were smoothed using a Gaussian filter (FWHM of 4.7 mm). Thus, we obtained maps for FA, RD, MD, and AD for each subject in normalized space.

Statistical analysis

Structural MRI data (T1- weighting) and the diffusion-weighted MRI data were analyzed in relation to diagnosis (ADHD and Controls) and the number of self-reported childhood and adult symptoms. For each of the six image series above, voxel-wise linear regression models were computed, for diagnosis (Control = 0, ADHD = 1), childhood and adulthood symptoms, and gender, as well as age at time of examination as covariates. For the independent variable grey matter (white matter) concentration, computation was restricted to a mask with a corresponding probability $p > 0.25$, for all other methods to a tissue mask with a white matter probability $p > 0.5$. As result, the significance of the regression coefficient for the regressor of interest was obtained as a voxel-wise z-score. Spatial clusters above an absolute z-score threshold of 2.5 (corresponding p-value of 0.01) were determined and assessed for significance ($p < 0.05$) based on the theory of excursion sets in Gaussian random fields [44]. This approach corrects for the multiple comparisons by controlling the family-wise error rate, and is based on the theory of Gaussian random fields. The cluster-extent based thresholding is currently the most popular method for multiple comparisons correction of statistical maps in neuroimaging studies, and is the commonly accepted standard in the context of voxel-based morphometry. Only clusters passing the significance test were reported. A voxel-level (primary) p-value threshold of $p = 0.01$ and a cluster-level (secondary) p-value threshold of $p = 0.05$ was used, which are standard settings for this approach. Average z-scores were computed over all voxels in a given cluster that passed the significance test. The center-of-mass, extent (in mm^3), peak and average z-score were computed for each cluster, and addressed an anatomical label based on Talairach coordinates using the labeled map developed by Lancaster et al. [45], and are compiled in tables.

In order to assess whether any combination of the subject-wise measures can be used to predict an ADHD diagnosis, we extracted voxel-wise measures from regions that significantly differed by the diagnostic label. For each subject and each analysis, continuous voxel-wise measures (GMC, WMC, JAC, FA, RD, MD) in significantly different regions were collected and averaged, resulting in one score per subject and analysis. Logistic regression was used to find a single score that best predicted an ADHD diagnosis. To assess the combined predictive power of all scores, we performed a principal component analysis (PCA) to reduce the dimensionality of the data, and used a linear discriminant analysis (LDA) to develop a simple classifier in the reduced space.

Results

ADHD diagnosis and brain structure

An ADHD diagnosis was associated with different grey (white) matter concentrations, and shape differences as computed from the Jacobian maps (JAC, see Table 2, S1, S2 and S3 Maps). The findings revealed: 1. regions of decreased grey matter in the right middle and inferior frontal gyrus, right superior and middle temporal gyrus, left caudate head, and left parahippocampal gyrus; 2. regions with increased white matter in the right frontal gyrus, right inferior frontal gyrus, right middle temporal gyrus, left and right external capsule, left internal capsule, and left parahippocampal gyrus; 3. regions with shape contractions (decreased JAC suggesting incomplete maturation) in the right middle frontal gyrus, right superior temporal gyrus, left middle temporal gyrus, right postcentral gyrus, left posterior insula, and left and right parahippocampal gyrus.

Table 2. Linear regression of model data DIAGNOSIS + AGE + SEX + ICV, assessing the importance of the diagnostic group on structural data.

		MNI Coordinates			Size		
Measurement/Structure		**x**	**y**	**z**	**mm^3**	**Z_{max}**	**Z_{av}**
Grey Matter							
	Right Middle Frontal Gyrus	29	35	34	376	-4.047	-2.883
	Right Inferior Frontal Gyrus	52	6	21	1383	-4.512	-3.024
	Right Superior Temporal Gyrus	52	-43	7	989	-4.245	-2.910
	Right Middle Temporal Gyrus	48	-65	15	584	-3.604	-2.871
	Left Caudate Head	-10	6	1	357	-3.483	-2.823
	Left Parahippocampal Gyrus	-24	-65	9	417	-3.821	-2.868
White Matter							
	Right Frontal Sub-Gyral WM	26	32	34	536	4.084	2.863
	Right Inferior Frontal Gyrus WM	49	6	23	1970	4.615	3.023
		46	39	7	348	3.502	2.777
	Right Middle Temporal Gyrus WM	52	-47	8	548	3.622	2.837
		49	-65	15	608	3.606	2.881
	Right External Capsule WM	25	6	13	896	3.394	2.770
	Left External Capsule WM	-23	13	19	450	3.620	2.826
	Left Internal Capsule	-9	-14	7	2910	3.930	2.856
	Left Parahippocampal Gyrus WM	-24	-65	9	715	4.134	2.953
	Pons	-3	-27	-36	562	3.286	2.761
Shape							
	Right Middle Frontal Gyrus WM	33	42	-2	650	-3.033	-2.680
		22	29	-15	592	-3.132	-2.710
	Right Superior Temporal Gyrus	30	10	-24	589	-2.923	-2.631
		51	-18	3	2382	-3.203	-2.685
	Left Middle Temporal Gyrus WM	-51	-33	-10	1649	-3.139	-2.709
	Right Postcentral Gyrus	42	-24	36	1345	-3.459	-2.857
	Left Posterior Insula	-45	-14	16	2544	-3.739	-2.874
	Left Parahippocampal Gyrus	-22	-59	7	551	-3.018	-2.652
		-12	-43	5	401	-2.927	-2.674
	Right Parahippocampal Gyrus	15	-59	11	3525	-3.144	-2.683

Regions with significant differences in GM & WM concentration, and shape (JAC) are shown, with their center position, size, peak, and mean z-score. The sign of the z-scores is given relative to controls. Positive (negative) z-scores correspond to a higher (lower) value of a specific variable in the ADHD group, e.g., a negative z-score to a lower grey matter concentration.

https://doi.org/10.1371/journal.pone.0175433.t002

Table 3 (S4, S5, S6 and S7 Maps) depicts the analysis of the DTI data analysis, which showed that an ADHD diagnosis is associated with: (1) regions of increased FA in the left external capsule, as well as left and right optic radiation; (2) regions of decreased FA in the right superior temporal gyrus, left and right middle temporal gyrus, right postcentral gyrus, cingulate gyrus, corpus callosum, left and right temporal stem, and right midbrain; (3) regions of increased RD, including the left and right postcentral gyrus, left middle temporal gyrus, cingulate gyrus, right internal capsule, and right midbrain; (4) regions of decreased RD, including the left supraventricular white matter and left pons; (5) regions of primarily increased MD in the left middle temporal white matter, right internal capsule, right midbrain, and left pons; (6) regions of decreased MD in the corpus callosum and left pons; (7) regions of increased AD in the right cuneus and right middle occipital gyrus; (8) regions of decreased AD in the right precentral

Table 3. Linear regression of model data DIAGNOSIS + AGE + SEX + ICV, assessing the importance of the diagnostic group on structural data.

		MNI Coordinates			Size		
Measurement/Structure		**x**	**y**	**z**	**mm^3**	**Z_{max}**	**Z_{av}**
Fractional Anisotropy							
	Left External Capsule	-29	-3	11	1229	4.050	3.057
	Left Optic Radiation	-33	-48	-6	1120	3.552	2.865
	Right Optic Radiation	20	-59	3	1369	3.838	2.864
	Right Pons	6	-21	-30	391	3.845	3.000
	Right Superior Temporal Gyrus	35	-59	29	753	-3.654	-2.906
	Left Middle Temporal Gyrus	-42	-58	6	553	-3.996	-2.986
	Right Middle Temporal Gyrus	44	-53	6	651	-3.816	-3.074
	Right Postcentral Gyrus	42	-31	37	1093	-3.889	-2.927
	Cingulate Gyrus	9	2	34	1264	-3.021	-2.668
		14	-36	35	429	-3.021	-2.668
	Corpus Callosum	4	-39	24	384	-2.957	-2.648
		-22	-81	19	1890	-4.785	-2.981
	Sub-Gyral WM	25	-21	54	514	-3.145	-2.705
		20	-55	51	556	-3.819	-2.967
		34	-14	29	1263	-4.030	-2.926
		-29	-21	30	504	-3.265	-2.793
		34	27	29	578	-3.722	-2.954
	Left Temporal Stem	-23	-54	23	1381	-3.879	-2.992
	Right Temporal Stem	24	-66	20	1739	-3.616	-2.843
	Right Midbrain	11	-24	-4	1929	-3.974	-2.781
Radial Diffusivity							
	Left Suptraventricular WM	-21	33	37	940	-3.504	-2.769
	Left Postcentral Gyrus	-40	-32	40	763	3.731	2.864
	Right Postcentral Gyrus	43	-32	34	379	3.619	2.860
	Left Middle Temporal Gyrus	-44	-59	2	651	4.376	3.168
	Cingulate Gyrus	9	-6	39	543	3.604	2.861
	Sub-Gyral WM	-34	-66	34	480	3.264	2.751
		-20	-85	28	551	3.879	2.920
		21	-92	14	562	4.211	2.958
		18	-86	26	1512	3.959	2.893
	Right Internal Capsule	6	-8	12	534	3.028	2.690
	Right Midbrain	4	-29	-6	620	3.245	2.792
Mean Diffusivity							
	Left Middle Temporal Gyrus WM	-45	-59	1	475	4.154	3.069
	Corpus Callosum	-18	-23	29	3006	-3.260	-2.673
		33	-57	15	509	-3.286	-2.785
		-31	-58	14	663	-3.366	-2.759
		-16	-71	5	412	-3.853	-2.931
	Sub-Gyral WM	17	-88	27	1156	3.849	2.867
		-18	-86	30	464	3.364	2.777
		21	-93	15	575	4.208	2.981
	Right Internal Capsule	5	-8	12	469	3.026	2.692
	Right Midbrain	3	-29	-6	533	3.242	2.782
Axial Diffusivity							
	Right Cuneus	18	-89	29	823	3.424	2.786

(*Continued*)

Table 3. (*Continued*)

Measurement/Structure		MNI Coordinates			Size		
		x	y	z	mm^3	Z_{max}	Z_{av}
	Right Middle Occipital Gyrus	21	-94	16	612	4.085	2.946
	Right Pre-central WM	34	-16	31	2417	-3.704	-2.961
	Left Occipital Lobe WM	-20	-43	26	6031	-3.707	-2.851
	Right Occipital Lobe WM	31	53	20	4041	-3.882	-2.912
	Right Brainstem	16	-22	-2	1039	-4.168	-2.893
	Left Brainstem	-16	-23	-9	361	-3.421	-2.785

Regions with significant differences in DTI measures FD, RD, MD, and AD are shown, with their center position, size, peak, and mean z-score. The sign of the z-scores is given relative to controls. Positive (negative) z-scores correspond to a higher (lower) value of a specific variable in the ADHD group.

https://doi.org/10.1371/journal.pone.0175433.t003

WM, occipital lobe, and brainstem. For an example overlay of brain areas that significantly differed in their WM properties due to ADHD, refer to Fig 1.

ADHD symptoms and brain structure

In contrast to diagnosis, no association was found between brain macrostructure and ADHD symptoms. However, ADHD symptoms were associated with microstructural findings, which were more prominent (i.e., number, size, and z-scores of significant regions) for the childhood total symptoms (see Table 4, S8, S9, S10 and S11 Maps), compared to the adult total symptoms (Table 5, S12, S13, S14 and S15 Maps). More specifically, the DTI analysis of the structural differences associated with childhood symptoms revealed: (1) a region of increased FA, RD and MD in the left sub-gyral white matter of the frontal lobe; (2) regions of increased RD and MD, including the right sub-gyral white matter of the frontal lobe and the left and right putamen and the adjacent external capsule; (3) a region of decreased RD and MD in the right superior temporal gyrus; (4) a region of decreased FA in the right putamen; (5) a region of decreased RD in the right medial frontal gyrus; (6) regions of increased AD in the right cingulate, frontal lobe, and left external capsule. The DTI analysis of the structural differences associated with adult symptoms revealed: (1) a region of decreased FA and increased RD in the right dentate nucleus; (2) a region of decreased FA, RD, MD, and AD in the left cingulum; (3) regions of increased FA, including the white matter of the right lingual gyrus, left putamen, and the white matter of the right temporo-occipital gyrus.

Morphometric data predicting ADHD diagnosis

Overall, a single measure of white matter concentration best predicted ADHD diagnosis ($p = 6.18e\text{-}06$). The receiver operating curve (ROC) analysis revealed that the "area under the curve" (AUC) was found at 0.917, which may be considered as a reasonably high discriminative power of this model. To assess the combined information of six measures (i.e., GM, WM, TBM, FA, RD, MD), PCA was used to reduce the dimensionality to three measures, representing a cumulative variance of 97.5%. Subsequent LDA to develop a simpler classifier correctly predicted an ADHD diagnosis in 83.3% of all cases (see Fig 2). A repeated random sub-sampling cross-validation with a 20% test set yielded a correct prediction rate of 81.4% (95% CI: 0.76–0.86).

Discussion

An ADHD diagnosis in young adults was associated with decreased grey matter concentration, increased white matter concentration, and decreased shape in widespread areas involving

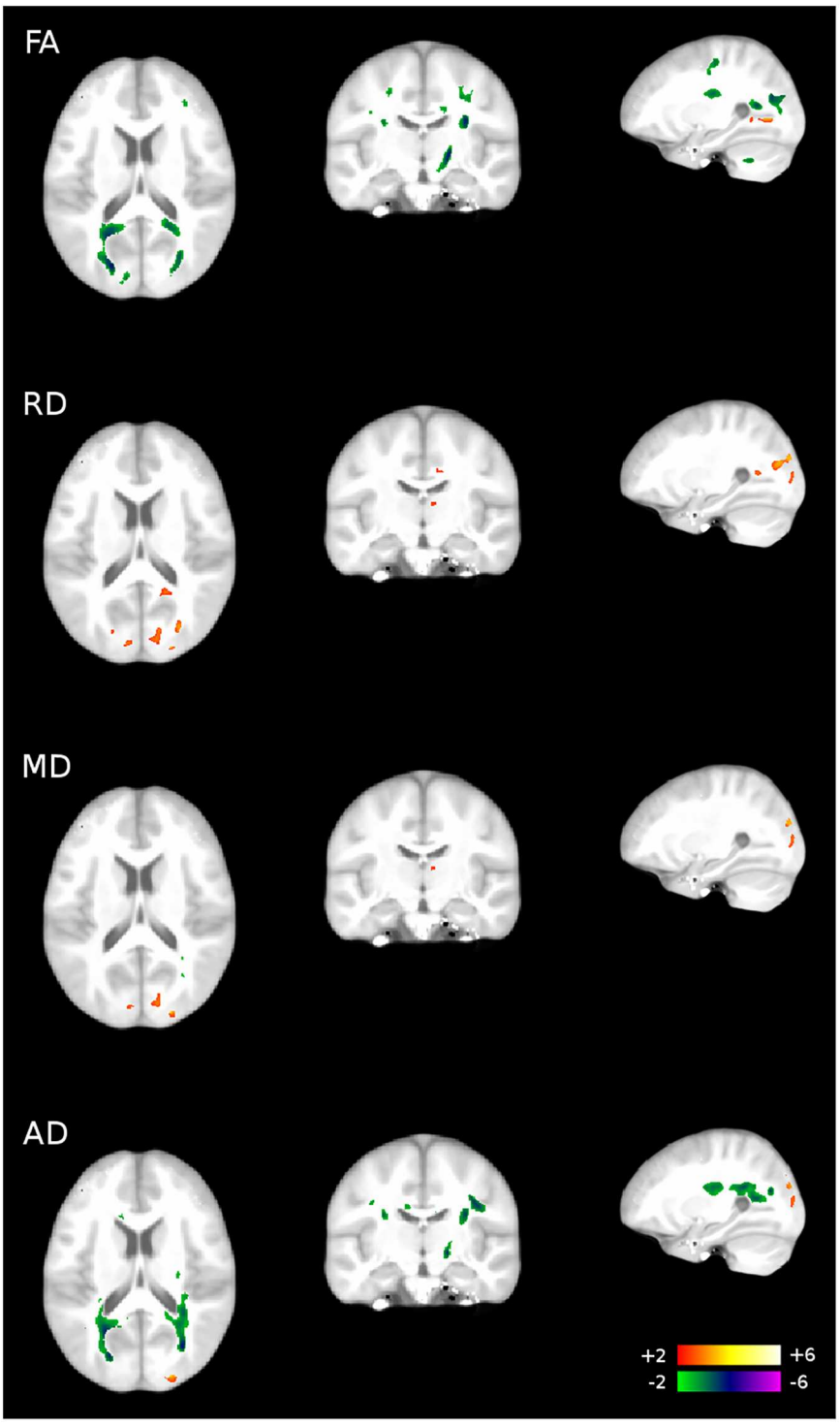

Fig 1. Overlay of brain areas that significantly differ in their WM properties due to ADHD diagnosis.

https://doi.org/10.1371/journal.pone.0175433.g001

frontal, temporal, striatal, parietal and limbic regions. These widespread macrostructural changes suggest that many of the brain areas associated with an ADHD diagnosis in childhood [16] continue to be affected in young adulthood. More specifically, an ADHD diagnosis in

Table 4. Linear regression of model data CHILDHOOD SYMPTOMS + AGE + SEX + ICV, assessing the importance of the total number of self-reported childhood symptoms on structural data.

		MNI Coordinates			Size		
Measurement/Structure		**x**	**y**	**z**	**mm^3**	**Z_{max}**	**Z_{av}**
Fractional Anisotropy							
	Left Sub-Gyral WM Frontal Lobe	-22	37	27	326	3.542	2.848
		-21	-11	51	644	3.723	2.944
		-24	1	47	415	3.523	2.887
	Right Putamen	21	0	7	458	-3.494	-2.786
Radial Diffusivity							
	Left Sub-Gyral WM Frontal Lobe	-17	29	-4	314	3.510	2.865
		-20	-10	54	328	-3.241	-2.751
	Right Sub-Gyral WM Frontal Lobe	20	-8	32	348	3.202	2.755
	Right Medial Frontal Gyrus	11	-12	64	516	-3.747	-2.888
	Right Superior Temporal Gyrus	42	4	-21	363	-3.636	-2.941
	Left Putamen/External Capsule	-27	3	9	1912	4.071	2.941
	Right Putamen/External Capsule	26	1	10	5301	4.158	3.061
Mean Diffusivity							
	Left Sub-Gyral WM Frontal Lobe	-26	6	28	1190	3.757	2.846
	Right Sub-Gyral WM Frontal Lobe	18	19	29	587	3.115	2.684
	Right Superior Temporal Gyrus WM	42	4	-20	359	-3.632	-2.994
	Left Putamen/External Capsule	-29	-24	26	2052	3.291	2.723
		-27	3	10	1687	3.693	2.833
	Right Putamen/External Capsule	26	-10	21	9069	4.269	2.875
Axial Diffusivity							
	Right Cingulate Gyrus	18	-21	46	1545	4.481	2.970
	Right Frontal Lobe WM	26	7	30	369	3.463	2.886
	Left Frontal Lobe WM	-27	5	28	551	3.726	2.854
	Left External Capsule	-31	8	11	772	3.857	2.832

Regions with significant differences in DTI measures FD, RD, MD, and AD are shown, with their center position, size, peak, and mean z-score. Positive (negative) z-scores correspond to a higher (lower) value of a specific variable in the ADHD group.

https://doi.org/10.1371/journal.pone.0175433.t004

young adults was associated with widespread changes to the maturation of white matter fiber bundles in the brain, such as structural shape changes (incomplete maturation) in the right middle frontal gyrus, right superior temporal gyrus, left middle temporal gyrus, right postcentral gyrus, left posterior insula, and bilateral parahippocampal gyrus. These incomplete maturations in frontal, temporal, parietal, and limbic structures are in agreement with previous findings on cerebral and cerebellar volumetric reductions associated with ADHD in children and adolescents [7, 46].

Our findings revealed reduced gray matter concentrations in the right middle frontal gyrus, right inferior frontal gyrus, right superior temporal gyrus, right middle temporal gyrus, left caudate head, and left parahippocampal gyrus with corresponding white matter increases associated with an ADHD diagnosis in young adults. Thus, frontal, temporal, striatal, parietal, and limbic abnormalities associated with ADHD are not unique to children and adolescents but are also seen in young adults, revealing that the pathophysiology of the disorder seen in childhood carries on into young adulthood. In addition, the reduced grey matter concentrations in the left caudate head in young adults with ADHD suggest that the macrostructural abnormalities in the basal ganglia may normalize at a later stage in adults with ADHD [7, 10, 24].

Table 5. Linear regression of model data ADULT SYMPTOMS + AGE + SEX + ICV, assessing the importance of the total number of self-reported adult symptoms on structural data.

		MNI Coordinates			Size		
Measurement/Structure		**x**	**y**	**z**	**mm^3**	**Z_{max}**	**Z_{av}**
Fractional Anisotropy							
	Right Lingual Gyrus WM	23	-59	1	411	3.689	2.902
	Left-Cingulum WM	-14	-68	13	564	-4.225	-3.138
	Left Putamen	-28	-17	11	784	3.907	2.921
	Right Temporo-Occipital Sub-Gyral WM	38	-68	-6	416	4.058	3.113
	Right Dentate Nucleus	3	-52	-26	1889	-4.695	-3.063
Radial Diffusivity							
	Left Cingulum	-23	-53	11	441	-4.184	-3.154
	Right Dentate Nucleus	5	-59	-18	384	3.272	2.778
Mean Diffusivity							
	Left Cingulum	-23	-53	11	537	-4.162	-3.109
Axial Diffusivity							
	Left Cingulum WM	-18	-54	18	1053	-4.171	-2.928

Regions with significant differences in DTI measures FD, RD, MD, and AD are shown, with their center position, size, peak, and mean z-score. Positive (negative) z-scores correspond to a higher (lower) value of a specific variable in the ADHD group.

https://doi.org/10.1371/journal.pone.0175433.t005

With regards to microstructural brain abnormalities, our findings corroborate an abnormal cortico-cortical connectivity that develops early and persists into young adulthood [17]. More specifically, increased MD in the left middle temporal gyrus, right internal capsule, and right midbrain suggests reduced white matter density and potential myelin breakdown associated with an adult ADHD diagnosis [4], which is in agreement with in increased MD found in previous studies in children and adolescents with ADHD [47]. Reduced FA and MD were found in the corpus callosum, which corroborates previous findings in children [48, 49] and adults with ADHD [50, 51]. The corpus callosum is central for communicating between different brain areas. Reduced white matter density in this structure may contribute significantly to brain network disturbances associated with ADHD. In addition, decreased FA in the right superior temporal gyrus and both sides of the middle temporal gyrus as well as decreased AD in the occipital lobe and brainstem were associated with an ADHD diagnosis. Low FA and AD values of the white matter may reflect axonal degeneration, and/or less well-organized tracts, and may be induced by a variety of influences [49]. Previous studies in children found increased FA for white matter structures connecting parietal-occipital regions and temporal lobes in children [52, 53]. Our results show that temporal lobes are also affected in size and connectivity in young adults with ADHD.

These DTI findings in young adults with an ADHD diagnosis are in agreement with recent data using whole-brain tractography [28], which revealed widespread disturbances in WM connectivity of children and adolescents involving frontal, striatal, and cerebellar brain regions. Similar to previous research, the dorsal striatum, in particular the putamen, showed regions with reduced FA on the right side and increased RD and MD on both sides including their cortico-striatal connections. The dorsal striatum mediates aspects of decision-making, in particular predicting consequences of goal-directed actions, which are impaired in individuals with ADHD [54]. In addition, increased RD was found in the postcentral gyrus, left middle temporal gyrus, cingulate gyrus, right internal capsule, and right midbrain suggesting decreased myelination or lower fiber density associated with an adult ADHD diagnosis.

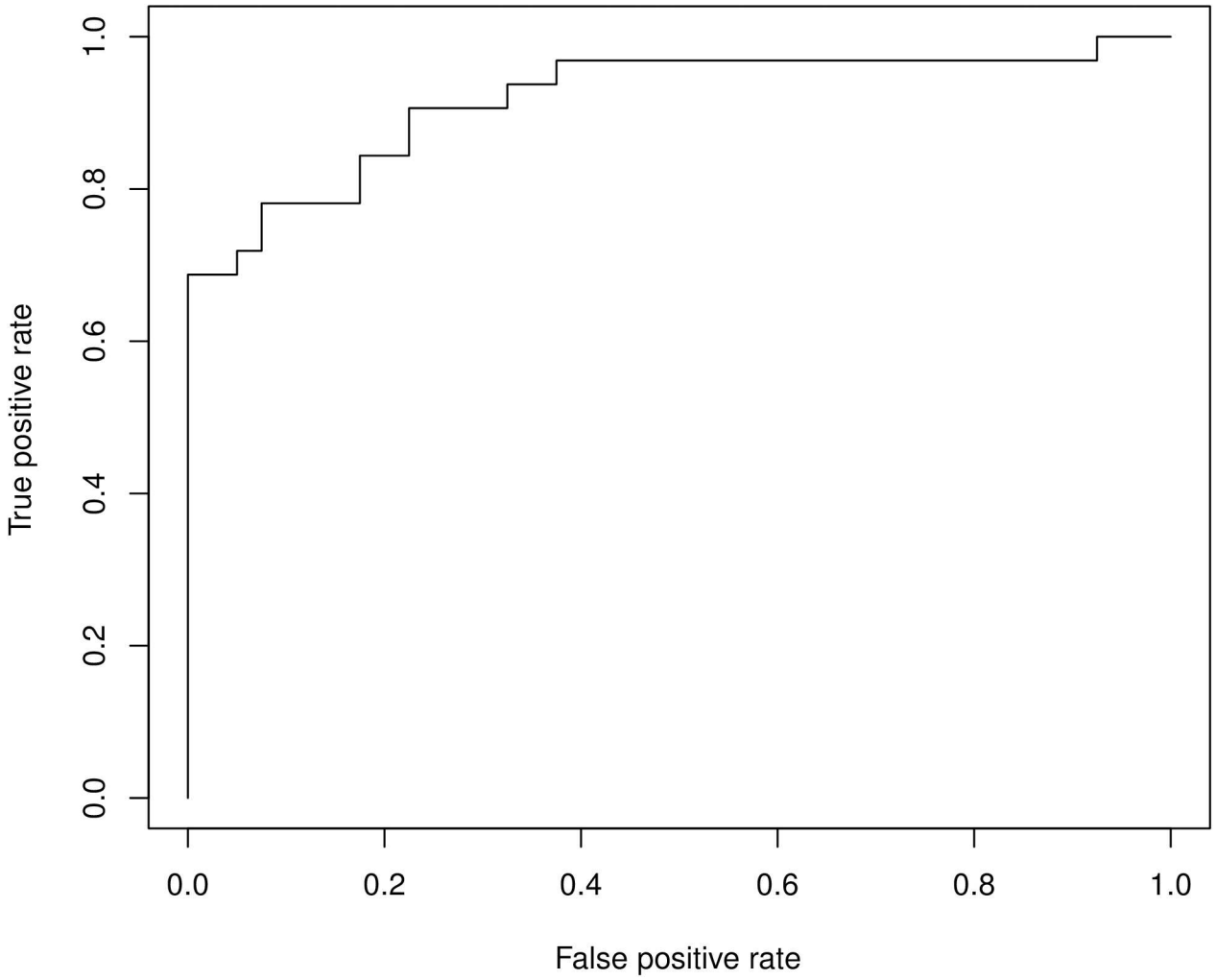

Fig 2. Receiver Operating Characteristics for predicting ADHD based on white matter density. The predictive power for the area under the curve is 0.917.

https://doi.org/10.1371/journal.pone.0175433.g002

Decreased connectivity and myelination in these areas may be a stable correlate for ADHD throughout the lifespan [55].

The present findings also corroborated the hypothesis that brain microstructural abnormalities were more associated with child symptoms of ADHD compared to adult symptoms of ADHD. More specifically, dividing into childhood and adult symptoms, the strongest associations between symptoms and morphometric findings were determined by the combination of self-reported childhood symptoms and diffusion-weighted measurements, but less so for childhood symptoms and T1- weighted measures. Although less prominent, a similar pattern was found for the adult symptoms. However, microstructural differences were more strongly associated with childhood than adult symptoms, which may suggest that while microstructural findings are strongly linked to childhood symptoms, such association weakens with adult ADHD symptoms, which may be due to improved structural changes or coping skills.

Intriguingly, childhood symptoms were associated with reduced FA and increased RD in the frontal lobe and putamen/external capsule, which suggests decreased myelination in the frontal–basal ganglia network. Adult symptoms, on the other hand, were associated with

reduced FA as well as increased RD and AD in the in the left cingulum and right dentate nucleus, suggesting decreased myelination in these structures in young adults with ADHD. These findings, in part, corroborate previous results of white matter differences associated with symptoms severity [15, 16, 21, 26, 55].

While reduced grey matter in the left caudate was associated with an ADHD diagnosis, reduced FA, as well as increased RD and MD in the left putamen, it was also correlated with child symptoms of ADHD, but not adult symptoms of ADHD. This suggests that disturbances in connections reaching the caudate may be associated with an ADHD diagnosis in young adulthood, whereas reduced FA in the putamen may be an index of symptom severity in childhood.

At the brain circuitry level, the present findings may suggest that the superior longitudinal fasciculus (SLF) and the cortico-limbic associated circuitry are dysfunctional in individuals with ADHD (see Fig 3). The SLF are longitudinal, intra-hemispheric, cortico-cortical bundles of myelinated axons that link the posterior and anterior cortices, including the frontal lobe to the anterior occipital as well as parietal and posterior temporal lobes. The SLF is primarily responsible for the visual and motor coordination, as well as spatial sense, language, and mirror neuron systems. There are several sections of the SLF with different functional contributions to behavior, which associate with the current anatomical findings. More specifically, the dorsal component of the SLF (SLF I) connects the dorsal and medial part of the frontal lobe (i.e., right middle frontal gyrus in Table 2) with the cingulate (Table 3) and cingulum (Table 5) of the superior and medial parietal cortex [56, 57]. As part of the dorsal attention network, the superior parietal cortex has lower connectivity in children with ADHD [58]. However, the SLF I codes primarily for location of body parts in a body-centered coordinate system and regulates higher aspects of motor behavior. Lesions in these regions have been associated with deficits selecting competing motor acts on the basis of appropriate conditional rules [59, 60]. The SLF II connects the middle frontal gyrus (Table 2) with the post central gyrus (Table 4) of the parietal lobe. The SLF II provides information on visual space and visuo-motor function, which may contribute to spatial attention [61–63]. Atypical functional coupling in parts of the SLF II has been associated with ADHD in a functional brain imaging study [64]. Such dysfunctional coupling may result in saccadic abnormalities, which have been found in children and adults with ADHD [65, 66]. The SLF III has been associated with language articulation and connects the rostral part of the inferior parietal lobule with the middle frontal gyrus, the inferior frontal gyrus (Table 2), and the frontal lobe (Table 5) [67]. The arcuate fasciculus and temporo-parietal section of the SLF connect the superior temporal gyrus (Tables 2, 3 and 4) with the prefrontal cortex, which modulates numerous language functions and audio-spatial information [67]. These findings may suggest complex audio-visual dysfunctions associated with ADHD [68–70].

The cortico-limbic associated circuitry connects the amygdala with the thalamus and orbital frontal cortex. It is primarily responsible for emotional learning and behavioral regulation. The present findings involving the caudate head (Table 2), parahippocampal gyrus (Table 2), cingulate gyrus (Table 3), cingulum (Table 5), putamen (Tables 4 and 5), and the external and internal capsule (Tables 2, 3, 4 and 5) suggest a link between cortico-limbic structures and ADHD in young adults. Such link corroborates that dysfunctional motivation, impulsivity, and emotionality may be major contributors to the disruptive behaviors associated with ADHD. A number of studies have shown that ADHD is associated with a motivational deficit due to a dopamine dysfunction in the basal ganglia [71–73]. Such motivational deficit is in agreement with parent reports of children with ADHD who can concentrate during interesting activities but are challenged by mundane and day-to-day tasks [74, 75]. Other studies have documented the comorbidity between ADHD and depression [76, 77]. However, it is yet to be determined if depression is an inherent part of ADHD or perhaps develops secondary in

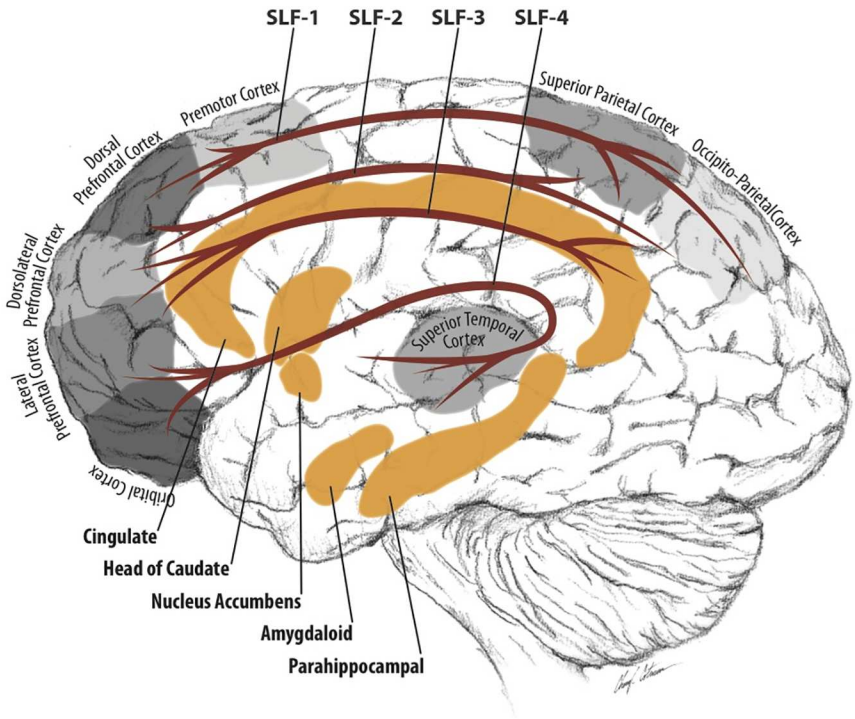

Fig 3. Brain circuitry associated with ADHD.

https://doi.org/10.1371/journal.pone.0175433.g003

young adults in response to the frustrations associated with not being able to focus as well as risky decision making or lifestyle. In any case, it is unlikely that comorbidities severely influenced the study findings because there were no significant differences in the comorbidities between the ADHD and control groups.

Intriguingly, MRI based data predicted the diagnosis of ADHD correctly in 83% of all the cases. Thus, further research towards defining a MRI-based biomarker is promising, which requires a larger and more diverse patient sample as well as an extended MRI protocol. Future studies could focus on the probability of certain areas and circuitries in predicting an ADHD diagnosis.

Limitations

The findings have to be interpreted with caution because childhood symptoms were assessed via self-report by young adults, which may be problematic due to memory bias or distortion. In addition, emerging evidence suggests that the ADHD inattentive and ADHD combined subtypes in children may be different disorders based on their unique WM microstructure [78], which was not taken into consideration in this study. Larger studies are needed to develop a better understanding of the anatomical differences between ADHD subtypes. Furthermore, while previous morphometric and DTI studies on white/gray matter integrity in adults with ADHD revealed deficits in structural connectivity, they may be not unique to ADHD [79]. Thus, more research is necessary to determine whether the morphometric findings presented here are specific to ADHD.

Conclusion

An adult ADHD diagnosis and in particular child symptoms were associated with widespread micro- and macrostructural changes in the frontal, basal ganglia, anterior cingulate, temporal,

and occipito-parietal regions in young adults with ADHD. The associations between brain structure and ADHD symptoms in childhood were more widespread and prominent (i.e., number, size, and z-scores of significant brain regions) than ADHD symptoms in adulthood. In addition, the analysis of the diffusion-weighted measures yielded stronger results (in terms of number, size, and z-scores of significant regions) than the measures derived from T1-weighted data. Thus, in relation to the diagnosis and symptom scores, changes in the microstructural properties of white matter fiber tracts appear to be stronger and more extensive than macrostructural differences. This highlights the importance of the microstructural architecture in the pathophysiology of ADHD.

The overall morphometric findings predict the ADHD diagnosis in 83% of cases, which demonstrates sufficient sensitivity to aid in the clinical assessment and potential as a biomarker for ADHD in young adults. At the brain circuitry level, the involvement of the SLF and cortico-limbic areas may suggest complex audio-visual, motivational, and emotional dysfunctions associated with ADHD in young adults, which could be investigated in future studies. Investigating the SLF and cortico-limbic circuitries may be an interesting and novel research direction, which may lead to a better understanding of the underlying mechanisms of ADHD and the development of novel treatments that target audio-visual, motivational, and emotional dysfunctions.

Supporting information

S1 Template. Study Specific Anatomical Template.
(GZ)

S1 Map. Grey Matter Map-Diagnosis.
(GZ)

S2 Map. White Matter-Diagnosis.
(GZ)

S3 Map. JAC Map-Diagnosis.
(GZ)

S4 Map. Fractional Anisotropy Map-Diagnosis.
(GZ)

S5 Map. Radial Diffusivity Map-Diagnosis.
(GZ)

S6 Map. Mean Diffusivity Map-Diagnosis.
(GZ)

S7 Map. Axial Diffusivity Map-Diagnosis.
(GZ)

S8 Map. Fractional Anisotropy Map-Childhood Symptoms.
(GZ)

S9 Map. Radial Diffusivity Map-Childhood Symptoms.
(GZ)

S10 Map. Mean Diffusivity Map-Childhood Symptoms.
(GZ)

S11 Map. Axial Diffusivity Map-Childhood Symptoms.
(GZ)

S12 Map. Fractional Anisotropy Map-Adult Symptoms.
(GZ)

S13 Map. Radial Diffusivity Map-Adult Symptoms.
(GZ)

S14 Map. Mean Diffusivity Map-Adult Symptoms.
(GZ)

S15 Map. Axial Diffusivity Map-Adult Symptoms.
(GZ)

Acknowledgments

Thanks for the generous financial support of The Center for Autism & Neurodevelopmental Disorders and Cheryl Cotman for graphics. All authors declare no financial interests or potential conflicts of interest.

Author Contributions

Conceptualization: JGG FK.

Data curation: FK.

Formal analysis: FK JGG.

Funding acquisition: JGG.

Investigation: JGG ET.

Methodology: JGG FK.

Project administration: JGG TT.

Resources: JGG LTM.

Software: FK LTM.

Supervision: JGG.

Validation: FK JGG.

Visualization: JGG FK.

Writing – original draft: JGG.

Writing – review & editing: JGG FK TT SDA ET LTM JF.

References

1. American Psychiatric Association. Diagnostic and Statistical Manual of Mental Disorders. 5th ed. Arlington, VA: American Psychiatric Association; 2013.
2. Faraone SV, Biederman J, Mick E. The age-dependent decline of attention deficit hyperactivity disorder: a meta-analysis of follow-up studies. Psychol Med. 2006 Feb 1; 36(02):159–65.
3. Song SK, Yoshino J, Le TQ, Lin SJ, Sun SW, Cross AH, et al. Demyelination increases radial diffusivity in corpus callosum of mouse brain. Neuroimage. 2005 May 15; 26(1):132–40. https://doi.org/10.1016/j.neuroimage.2005.01.028 PMID: 15862213

4. Alexander AL, Lee JE, Lazar M, Field AS. Diffusion tensor imaging of the brain. Neurotherapeutics. 2007 July 31; 4(3):316–29. https://doi.org/10.1016/j.nurt.2007.05.011 PMID: 17599699
5. Tievsky AL, Ptak T, Farkas J. Investigation of apparent diffusion coefficient and diffusion tensor anisotropy in acute and chronic multiple sclerosis lesions. AJNR Am J Neuroradiol. 1999 Sep 1; 20(8):1491–9. PMID: 10512236
6. Song SK, Sun SW, Ramsbottom MJ, Chang C, Russell J, Cross AH. Dysmyelination revealed through MRI as increased radial (but unchanged axial) diffusion of water. Neuroimage. 2002 Nov 30; 17 (3):1429–36. PMID: 12414282
7. Castellanos FX, Lee PP, Sharp W, Jeffries NO, Greenstein DK, Clasen LS, et al. Developmental trajectories of brain volume abnormalities in children and adolescents with attention-deficit/hyperactivity disorder. J Am Med Assoc. 2002 Oct 9; 288(14):1740–8.
8. Valera EM, Faraone SV, Murray KE, Seidman LJ. Meta-analysis of structural imaging findings in attention-deficit/hyperactivity disorder. Biol Psychiatry. 2007 Jun 15; 61(12):1361–9. https://doi.org/10.1016/j.biopsych.2006.06.011 PMID: 16950217
9. Ellison-Wright I, Ellison-Wright Z, Bullmore E. Structural brain change in attention deficit hyperactivity disorder identified by meta-analysis. BMC psychiatry. 2008 Jun 30; 8(1):51.
10. Frodl T, Skokauskas N. Meta-analysis of structural MRI studies in children and adults with attention deficit hyperactivity disorder indicates treatment effects. Acta Psychiatr Scand. 2012 Feb 1; 125(2):114–26. https://doi.org/10.1111/j.1600-0447.2011.01786.x PMID: 22118249
11. Nakao T, Radua J, Rubia K, Mataix-Cols D. Gray matter volume abnormalities in ADHD: voxel-based meta-analysis exploring the effects of age and stimulant medication. Am J Psychiatry. 2011 Nov; 168 (11):1154–63. https://doi.org/10.1176/appi.ajp.2011.11020281 PMID: 21865529
12. Amico F, Stauber J, Koutsouleris N, Frodl T. Anterior cingulate cortex gray matter abnormalities in adults with attention deficit hyperactivity disorder: a voxel-based morphometry study. Psychiatry Res. 2011 Jan 30; 191(1):31–5. https://doi.org/10.1016/j.pscychresns.2010.08.011 PMID: 21129938
13. Bush G, Valera EM, Seidman LJ. Functional neuroimaging of attention-deficit/hyperactivity disorder: a review and suggested future directions. Biol Psychiatry. 2005 June 1; 57(11):1273–84. https://doi.org/10.1016/j.biopsych.2005.01.034 PMID: 15949999
14. Fan J, Posner M. Human attentional networks. Psychiatr Prax. 2004 Nov; 31 Suppl 2:S210–4.
15. Nagel BJ, Bathula D, Herting M, Schmitt C, Kroenke CD, Fair D, et al. Altered white matter microstructure in children with attention-deficit/hyperactivity disorder. J Am Acad Child Adolesc Psychiatry. 2011 Mar 31; 50(3):283–92. https://doi.org/10.1016/j.jaac.2010.12.003 PMID: 21334568
16. van Ewijk H, Heslenfeld DJ, Zwiers MP, Buitelaar JK, Oosterlaan J. Diffusion tensor imaging in attention deficit/hyperactivity disorder: A systematic review and meta-analysis. Neurosci Biobehav Rev. 2012 Apr 30; 36(4):1093–106. https://doi.org/10.1016/j.neubiorev.2012.01.003 PMID: 22305957
17. Liston C, Cohen MM, Teslovich T, Levenson D, Casey BJ. Atypical prefrontal connectivity in attention-deficit/hyperactivity disorder: pathway to disease or pathological end point?. Biol Psychiatry. 2011 Jun 15; 69(12):1168–77. https://doi.org/10.1016/j.biopsych.2011.03.022 PMID: 21546000
18. Makris N, Buka SL, Biederman J, Papadimitriou GM, Hodge SM, Valera EM, et al. Attention and executive systems abnormalities in adults with childhood ADHD: a DT-MRI study of connections. Cereb Cortex. 2008 May 1; 18(5):1210–20. https://doi.org/10.1093/cercor/bhm156 PMID: 17906338
19. Konrad A, Dielentheis TF, El Masri D, Bayerl M, Fehr C, Gesierich T, et al. Disturbed structural connectivity is related to inattention and impulsivity in adult attention deficit hyperactivity disorder. Eur J Neurosci. 2010 Mar 1; 31(5):912–9. https://doi.org/10.1111/j.1460-9568.2010.07110.x PMID: 20374289
20. Rüsch N, Weber M, Il'yasov KA, Lieb K, Ebert D, Hennig J, t al. Inferior frontal white matter microstructure and patterns of psychopathology in women with borderline personality disorder and comorbid attention-deficit hyperactivity disorder. Neuroimage. 2007 Apr 1; 35(2):738–47. https://doi.org/10.1016/j.neuroimage.2006.12.007 PMID: 17289404
21. Ashtari M, Kumra S, Bhaskar SL, Clarke T, Thaden E, Cervellione KL, et al. Attention-deficit/hyperactivity disorder: a preliminary diffusion tensor imaging study. Biol Psychiatry. 2005 Mar 1; 57(5):448–55. https://doi.org/10.1016/j.biopsych.2004.11.047 PMID: 15737658
22. Konrad A, Dielentheis TF, El Masri D, Dellani PR, Stoeter P, Vucurevic G, et al. White matter abnormalities and their impact on attentional performance in adult attention-deficit/hyperactivity disorder. Eur Arch Psychiatry Clin Neurosci. 2012 Jun 1; 262(4):351–60. https://doi.org/10.1007/s00406-011-0251-1 PMID: 21879383
23. Alexander GE, DeLong MR, Strick PL. Parallel organization of functionally segregated circuits linking basal ganglia and cortex. Annu Rev Neurosci. 1986 Mar; 9(1):357–81.

24. Lahey BB, Van Hulle CA, Singh AL, Waldman ID, Rathouz PJ. Higher-order genetic and environmental structure of prevalent forms of child and adolescent psychopathology. AMA Arch Gen Psychiatry. 2011 Feb 7; 68(2):181–9.

25. De La Fuente A, Xia S, Branch C, Li X. A review of attention-deficit/hyperactivity disorder from the perspective of brain networks. Front Hum Neurosci. 2013; 7:192. https://doi.org/10.3389/fnhum.2013.00192 PMID: 23720619

26. Shang CY, Wu YH, Gau SS, Tseng WY. Disturbed microstructural integrity of the frontostriatal fiber pathways and executive dysfunction in children with attention deficit hyperactivity disorder. Psychol Med. 2013 May 1; 43(05):1093–107.

27. Arnsten AF. Fundamentals of attention-deficit/hyperactivity disorder: circuits and pathways. J Clin Psychiatry. 2005 Dec; 67:7–12.

28. Hong SB, Zalesky A, Fornito A, Park S, Yang YH, Park MH, et al. Connectomic disturbances in attention-deficit/hyperactivity disorder: a whole-brain tractography analysis. Biol Psychiatry. 2014 Oct 15; 76 (8):656–63. https://doi.org/10.1016/j.biopsych.2013.12.013 PMID: 24503470

29. Bramham J, Murphy DG, Xenitidis K, Asherson P, Hopkin G, Young S. Adults with attention deficit hyperactivity disorder: an investigation of age-related differences in behavioural symptoms, neuropsychological function and co-morbidity. Psychol Med. 2012 Oct 1; 42(10):2225–34. https://doi.org/10.1017/S0033291712000219 PMID: 22369977

30. American Psychiatric Association. Diagnostic and Statistical Manual of Mental Disorders. 4th ed. Arlington, VA: American Psychiatric Association; 2000.

31. Gehricke J-G, Hong N, Whalen CK, Steinhoff K, Wigal TL. Effects of transdermal nicotine on symptoms, moods, and cardiovascular activity in the everyday lives of smokers and nonsmokers with attention-deficit/hyperactivity disorder. Psychol Addict Behav 2009 Dec; 23(4):644. https://doi.org/10.1037/a0017441 PMID: 20025370

32. Gehricke J-G, Hong N, Wigal TL, Chan V, Doan A. ADHD medication reduces cotinine levels and withdrawal in smokers with ADHD. Pharmacol Biochem Behav. 2011 May 31; 98(3):485–91. https://doi.org/10.1016/j.pbb.2011.02.021 PMID: 21356232

33. Ly C, Gehricke J-G. Marijuana use is associated with inattention in men and sleep quality in women with Attention-Deficit/Hyperactivity Disorder: A preliminary study. Psychiatry Res. 2013 Dec 30; 210 (3):1310–2. https://doi.org/10.1016/j.psychres.2013.08.003 PMID: 23993465

34. Gehricke J-G, Polzonetti C, Caburian C, Gratton E. Prefrontal hemodynamic changes during cigarette smoking in young adult smokers with and without ADHD. Pharmacol Biochem Behav. 2013 Nov 1; 112:78–81. https://doi.org/10.1016/j.pbb.2013.10.001 PMID: 24125785

35. First MB, Gibbon M, Spitzer RL, Williams JB. User's guide for the structured interview for DSM-IV axis I disorders—research version (SCID-I, version 2.0, February 1996 final version). New York: Biometrics Research. 1996 Feb.

36. Wigal T, Wigal SB, Steinhoff K, Kollins S, Newcorn JH, Steinberg-Epstein R, et al. Establishing a clinical diagnosis of ADHD in adults: the QUEST method. Advances in ADHD. 2007; 2:17–24.

37. Mehringer AM, Downey KK, Schuh LM, Pomerleau CS, Snedecor SM, Schubiner H. The Assessment of Hyperactivity and Attention: Development and preliminary validation of a brief self-assessment of adult ADHD. J Atten Disord. 2001 Nov; 5(4):223–31.

38. Kruggel F, von Cramon DY. Alignment of magnetic-resonance brain datasets with the stereotactical coordinate system. Med Image Anal. 1999 Jun 1; 3(2):175–85. PMID: 10711997

39. Fonov V, Evans AC, Botteron K, Almli CR, McKinstry RC, Collins DL, Brain Development Cooperative Group. Unbiased average age-appropriate atlases for pediatric studies. Neuroimage. 2011 Jan 1; 54 (1):313–27. https://doi.org/10.1016/j.neuroimage.2010.07.033 PMID: 20656036

40. Vercauteren T, Pennec X, Perchant A, Ayache N. Diffeomorphic demons: Efficient non-parametric image registration. Neuroimage. 2009 Mar 31; 45(1):S61–72.

41. Hentschel S, Kruggel F. Determination of the intracranial volume: a registration approach. International Workshop on Medical Imaging and Virtual Reality 2004 Aug 19 (pp. 253–260). Springer Berlin Heidelberg.

42. Zhang S, Arfanakis K. Role of standardized and study-specific human brain diffusion tensor templates in inter-subject spatial normalization. J Magn Reson Imaging. 2013 Feb 1; 37(2):372–81. https://doi.org/10.1002/jmri.23842 PMID: 23034880

43. Fillard P, Pennec X, Arsigny V, Ayache N. Clinical DT-MRI estimation, smoothing, and fiber tracking with log-Euclidean metrics. IEEE Trans Med Imaging. 2007 Nov; 26(11):1472–82. https://doi.org/10.1109/TMI.2007.899173 PMID: 18041263

44. Friston KJ, Worsley KJ, Frackowiak RS, Mazziotta JC, Evans AC. Assessing the significance of focal activations using their spatial extent. Hum Brain Mapp. 1994 Jan 1; 1(3):210–20. https://doi.org/10.1002/hbm.460010306 PMID: 24578041

45. Lancaster JL, Tordesillas-Gutiérrez D, Martinez M, Salinas F, Evans A, Zilles K, et al. Bias between MNI and Talairach coordinates analyzed using the ICBM-152 brain template. Hum Brain Mapp. 2007 Nov 1; 28(11):1194–205. https://doi.org/10.1002/hbm.20345 PMID: 17266101

46. Carmona S, Vilarroya O, Bielsa A, Tremols V, Soliva JC, Rovira M, et al. Global and regional gray matter reductions in ADHD: a voxel-based morphometric study. Neurosci Lett. 2005 Dec 2; 389(2):88–93. https://doi.org/10.1016/j.neulet.2005.07.020 PMID: 16129560

47. Lawrence KE, Levitt JG, Loo SK, Ly R, Yee V, O'Neill J, et al. White matter microstructure in subjects with attention-deficit/hyperactivity disorder and their siblings. J Am Acad Child Adolesc Psychiatry. 2013 Apr 30; 52(4):431–40. https://doi.org/10.1016/j.jaac.2013.01.010 PMID: 23582873

48. Cao Q, Sun L, Gong G, Lv Y, Cao X, Shuai L, et al. The macrostructural and microstructural abnormalities of corpus callosum in children with attention deficit/hyperactivity disorder: a combined morphometric and diffusion tensor MRI study. Brain Res. 2010 Jan 15; 1310:172–80. https://doi.org/10.1016/j.brainres.2009.10.031 PMID: 19852946

49. Qiu MG, Ye Z, Li QY, Liu GJ, Xie B, Wang J. Changes of brain structure and function in ADHD children. Brain Topogr. 2011 Oct 1; 24(3–4):243–52. https://doi.org/10.1007/s10548-010-0168-4 PMID: 21191807

50. Dramsdahl M, Westerhausen R, Haavik J, Hugdahl K, Plessen KJ. Adults with attention-deficit/hyperactivity disorder—a diffusion-tensor imaging study of the corpus callosum. Psychiatry Res. 2012 Feb 28; 201(2):168–73. https://doi.org/10.1016/j.pscychresns.2011.08.005 PMID: 22386969

51. Onnink AM, Zwiers MP, Hoogman M, Mostert JC, Dammers J, Kan CC, et al. Deviant white matter structure in adults with attention-deficit/hyperactivity disorder points to aberrant myelination and affects neuropsychological performance. Prog Neuropsychopharmacol Biol Psychiatry. 2015 Dec 3; 63:14–22. https://doi.org/10.1016/j.pnpbp.2015.04.008 PMID: 25956761

52. Silk TJ, Vance A, Rinehart N, Bradshaw JL, Cunnington R. White-matter abnormalities in attention deficit hyperactivity disorder: a diffusion tensor imaging study. Hum brain Mapp. 2009 Sep 15; 30(9):2757–65. https://doi.org/10.1002/hbm.20703 PMID: 19107752

53. Peterson DJ, Ryan M, Rimrodt SL, Cutting LE, Denckla MB, Kaufmann WE, et al. Increased regional fractional anisotropy in highly screened attention-deficit hyperactivity disorder (ADHD). J Child Neurol. 2011 Oct; 26(10):1296–302. https://doi.org/10.1177/0883073811405662 PMID: 21628699

54. Balleine BW, Delgado MR, Hikosaka O. The role of the dorsal striatum in reward and decision-making. J Neurosci. 2007 Aug 1; 27(31):8161–5. https://doi.org/10.1523/JNEUROSCI.1554-07.2007 PMID: 17670959

55. Shaw P, Sudre G, Wharton A, Weingart D, Sharp W, Sarlls J. White matter microstructure and the variable adult outcome of childhood attention deficit hyperactivity disorder. Neuropsychopharmacology. 2015 Feb 1; 40(3):746–54. https://doi.org/10.1038/npp.2014.241 PMID: 25241803

56. Lacquaniti F, Guigon E, Bianchi L, Ferraina S, Caminiti R. Representing spatial information for limb movement: role of area 5 in the monkey. Cereb cortex. 1995 Sep 1; 5(5):391–409. PMID: 8547787

57. Mountcastle VB, Lynch JC, Georgopoulos A, Sakata H, Acuna C. Posterior parietal association cortex of the monkey: command functions for operations within extrapersonal space. J Neurophysiol. 1975 Jul 1; 38(4):871–908. PMID: 808592

58. Tomasi D, Volkow ND. Abnormal functional connectivity in children with attention-deficit/hyperactivity disorder. Biol Psychiatry. 2012 Mar 1; 71(5):443–50. https://doi.org/10.1016/j.biopsych.2011.11.003 PMID: 22153589

59. Milner B, Petrides M. Behavioural effects of frontal-lobe lesions in man. Trends Neurosci. 1984 Nov 30; 7(11):403–7.

60. Halsband U, Passingham R. The role of premotor and parietal cortex in the direction of action. Brain Res. 1982 May 27; 240(2):368–72. PMID: 7104700

61. Mesulam M. A cortical network for directed attention and unilateral neglect. Ann Neurol. 1981 Oct 1; 10 (4):309–25. https://doi.org/10.1002/ana.410100402 PMID: 7032417

62. Posner MI, Walker JA, Friedrich FJ, Rafal RD. Effects of parietal injury on covert orienting of attention. J Neurosci. 1984 Jul 1; 4(7):1863–74. PMID: 6737043

63. Bisley JW, Goldberg ME. Neuronal activity in the lateral intraparietal area and spatial attention. Science. 2003 Jan 3; 299(5603):81–6. https://doi.org/10.1126/science.1077395 PMID: 12511644

64. Franzen JD, Heinrichs-Graham E, White ML, Wetzel MW, REEGT NL. Atypical coupling between posterior regions of the default mode network in attention-deficit/hyperactivity disorder: a pharmaco-

magnetoencephalography study. J Psychiatry Neurosci. 2013 Sep 1; 38(5):333. https://doi.org/10.1503/jpn.120054 PMID: 23611175

65. Matsuo Y, Watanabe M, Taniike M, Mohri I, Kobashi S, Tachibana M, et al. Gap effect abnormalities during a visually guided pro-saccade task in children with attention deficit hyperactivity disorder. PloS One. 2015 May 27; 10(5):e0125573. https://doi.org/10.1371/journal.pone.0125573 PMID: 26018057

66. Fried M, Tsitsiashvili E, Bonneh YS, Sterkin A, Wygnanski-Jaffe T, Epstein T, et al. ADHD subjects fail to suppress eye blinks and microsaccades while anticipating visual stimuli but recover with medication. Vision Res. 2014 Aug 31; 101:62–72. https://doi.org/10.1016/j.visres.2014.05.004 PMID: 24863585

67. Petrides M, Pandya DN. Comparative cytoarchitectonic analysis of the human and the macaque ventrolateral prefrontal cortex and corticocortical connection patterns in the monkey. Eur J Neurosci. 2002 Jul 1; 16(2):291–310. PMID: 12169111

68. Hawk LW, Yartz AR, Pelham WE, Lock TM. The effects of methylphenidate on prepulse inhibition during attended and ignored prestimuli among boys with attention-deficit hyperactivity disorder. Psychopharmacology. 2003 Jan 18; 165(2):118–27. https://doi.org/10.1007/s00213-002-1235-7 PMID: 12417963

69. Kim S, Chen S, Tannock R. Visual function and color vision in adults with Attention-Deficit/Hyperactivity Disorder. J Optom. 2014 Mar 31; 7(1):22–36. https://doi.org/10.1016/j.optom.2013.07.001 PMID: 24646898

70. Werner J, Weisbrod M, Resch F, Roessner V, Bender S. Increased performance uncertainty in children with ADHD?-Elevated post-imperative negative variation (PINV) over the ventrolateral prefrontal cortex. Behav Brain Funct. 2011 Aug 25; 7(1):38.

71. Volkow ND, Wang GJ, Kollins SH, Wigal TL, Newcorn JH, Telang F, et al. Evaluating dopamine reward pathway in ADHD: clinical implications. J Am Med Assoc. 2009 Sep 9; 302(10):1084–91.

72. Volkow ND, Wang GJ, Newcorn J, Fowler JS, Telang F, Solanto MV, et al. Brain dopamine transporter levels in treatment and drug naive adults with ADHD. Neuroimage. 2007 Feb 1; 34(3):1182–90. https://doi.org/10.1016/j.neuroimage.2006.10.014 PMID: 17126039

73. Volkow ND, Wang GJ, Tomasi D, Kollins SH, Wigal TL, Newcorn JH, et al. Methylphenidate-elicited dopamine increases in ventral striatum are associated with long-term symptom improvement in adults with attention deficit hyperactivity disorder. J Neurosci. 2012 Jan 18; 32(3):841–9. https://doi.org/10.1523/JNEUROSCI.4461-11.2012 PMID: 22262882

74. Barkley RA, Murphy KR. The nature of executive function (EF) deficits in daily life activities in adults with ADHD and their relationship to performance on EF tests. J Psychopathol Behav Assess. 2011 Jun 1; 33(2):137–58.

75. Volkow ND, Wang GJ, Newcorn JH, Kollins SH, Wigal TL, Telang F, et al. Motivation deficit in ADHD is associated with dysfunction of the dopamine reward pathway. Mol Psychiatry. 2011 Nov 1; 16(11):1147–54. https://doi.org/10.1038/mp.2010.97 PMID: 20856250

76. Biederman J, Ball SW, Monuteaux MC, Mick E, Spencer TJ, McCREARY MI, et al. New insights into the comorbidity between ADHD and major depression in adolescent and young adult females. J Am Acad Child Adolesc Psychiatry. 2008 Apr 30; 47(4):426–34. https://doi.org/10.1097/CHI.0b013e31816429d3 PMID: 18388760

77. Jensen PS, Hinshaw SP, Kraemer HC, Lenora N, Newcorn JH, Abikoff HB, et al. ADHD comorbidity findings from the MTA study: comparing comorbid subgroups. J Am Acad Child Adolesc Psychiatry. 2001 Feb 28; 40(2):147–58. https://doi.org/10.1097/00004583-200102000-00009 PMID: 11211363

78. Svatkova A, Nestrasil I, Rudser K, Goldenring Fine J, Bledsoe J, Semrud-Clikeman M. Unique white matter microstructural patterns in ADHD presentations—a diffusion tensor imaging study. Hum Brain Mapp. 2016 Sep 1; 37(9):3323–36. https://doi.org/10.1002/hbm.23243 PMID: 27159198

79. Davenport ND, Karatekin C, White T, Lim KO. Differential fractional anisotropy abnormalities in adolescents with ADHD or schizophrenia. Psychiatry Res. 2010 Mar 30; 181(3):193–8. https://doi.org/10.1016/j.pscychresns.2009.10.012 PMID: 20153608